Water and **Environment** Journal
Promoting Sustainable Solutions

Water and Environment Journal. Print ISSN 1747-6585

TECHNICAL NOTE

Composite hydrogeological investigation and characterisation methods applied at a nuclear power plant site in Taiwan

Hung-Chieh Lo, Po-Yi Chou, Chun-Chieh Huang, Po-Jui Chen & Shih-Meng Hsu

Geotechnical Engineering Research Center, Sinotech Engineering Consultants, Inc., Taipei, Taiwan

Keywords
borehole geophysical log; environmental impact assessment; hydrogeological characterisation; pumping test; tracer test.

Correspondence
Hung-Chieh Lo, Geotechnical Engineering Research Center, Sinotech Engineering Consultants, Inc., 7, Lane 26, Yat-Sen Road, Taipei 110, Taiwan. Email: jaylo@sinotech.org.tw

doi:10.1111/wej.12041

Abstract

Drawing from the lessons learnt from the Fukushima nuclear disaster in Japan, the assessment of subsurface environmental hazard around nuclear power plants has emerged as a critical task. Consequently, aiming to better understand the possible environmental impact of radiation leaks into the groundwater, a prescreening programme was initiated in 2011 by the Taiwanese government. As part of this programme, this study conducted various borehole prospecting techniques to identify *in situ* hydrogeological characteristics at Chin-Shan Nuclear Power Plant. Borehole electrical log, sonic log and temperature/conductivity log were conducted to explain the regional lithologic conditions and permeability of the formation. In conjunction with this, the interwell tracer and pumping test was carried out to simultaneously determine the hydraulic parameters. In our opinion, the implementation of such *in situ* end-to-end investigations is essential in interpreting *in situ* fluid and solute transport dynamics prior to programming any numerical scheme for early warning, vulnerability assessment and regular monitoring of a nuclear power plant site.

Introduction

Growing concern has been voiced in the general public about the environmental impact of effluent and leachate from landfills, coal mines, abandoned dumps, waste-storage tanks and, particularly, radioactive waste disposal sites. Drawing from the lessons learnt from the 2011 Fukushima nuclear disaster in Japan, an early-warning scheme and a robust action plan are definitely required to promptly eliminate any possible threat caused by the leakage of hazardous substances. Particularly for neighbouring and geographically proximate countries, such as Taiwan, where groundwater plays a major role in domestic supply and food security, insights regarding aquifer hydraulic properties near nuclear power plants are becoming the primary environmental concern of local governments. Commonly, to revisit and improve the understanding of regional groundwater dynamics, the use of a numerical model is a recognised approach. However, the uncertainty of hydrogeological properties in the model is often the major factor affecting the accuracy of the estimate and project implementation.

To increase the reliability and confidence in the use of numerical models, a thorough hydrogeological investigation and *in situ* controlled experiments prior to the final decision are essential (Buchanan *et al*. 2001; Ku *et al*. 2009; Hsu *et al*. 2010, 2011) to provide a crucial guideline in clarifying the complexity of the subsurface environment. Moreover, for the investigation of a nuclear power plant site, particularly if it is located in a geologically sensitive area, the usefulness of the chosen techniques and the *in situ* environmental conditions must be carefully considered. By integrating different borehole geophysical measurements and interwell pumping and tracer test, the purpose of this study is to gain more insight into the hydrogeological characteristics around the Chin-Shan Nuclear Power Plant (CSNPP, the first nuclear power plant in Taiwan, which started commercial operation in 1978), such as the regional geological conditions, stratum permeability and hydraulic parameters. The considerations, approaches and findings of the investigation are described in this paper.

Background information

The CSNPP is located at the most northerly part of the western foothills of Taiwan, at a latitude and longitude of 25°17′N and 121°35′E, respectively. The elevation is about 70 m above sea level, and the topographic slope is 30° from the south towards the north. The site is overlain by Pleistocene (Quaternary) deposits. Gravel deposits are found near the surface, while the predominant lithologies in the deeper formation are composed of clayey sandstone and sandstone-shale alternations. According to the statistical data of the

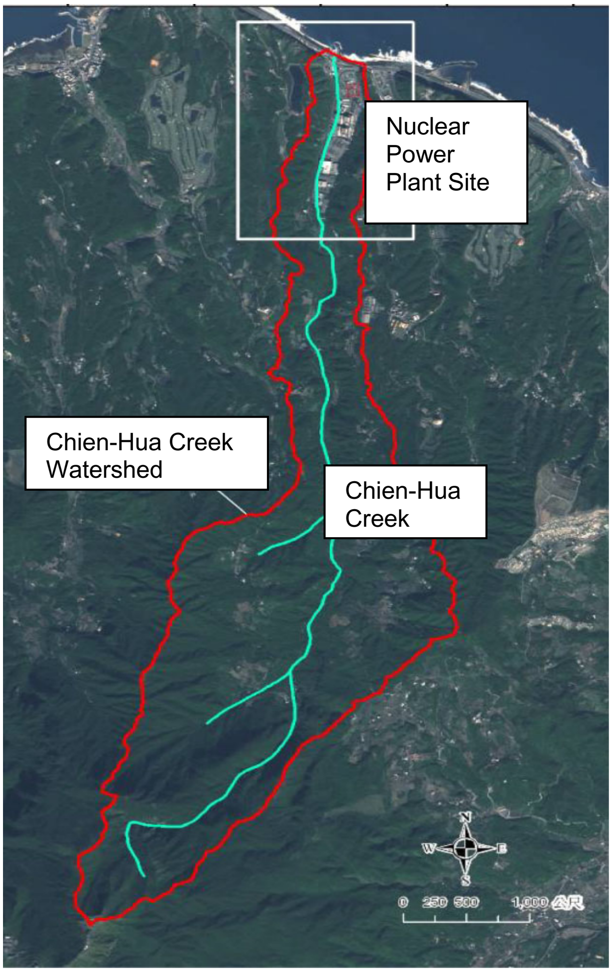

Fig. 1. Remote sensing image of the Chien-Hua Creek Watershed (Sinotech Engineering Consultants, Ltd. 2009).

Central Weather Bureau in Taiwan, the site receives an average 65.6 mm/day of precipitation from January to April, while higher precipitation, around 79.2 mm/day, is recorded during the rainy season from May to December. CSNPP is located downstream of the Chien-Hua Creek watershed. Flowing from the Jutz Mountain (1053 m above sea level), the drainage area of the Chien-Hua Creek watershed is approximately 8.82 square kilometres. As can be seen in Fig. 1, the creek is the only drainage in the region, passing through the left side of CSNPP. According to the site investigation report by Sinotech Engineering Consultants, Ltd. in 2009, the direction of the shallow groundwater flow across the site runs in a south–north direction. It is evident that the downstream coastal aquifers are at immediate risk once leachate enters the groundwater (Sinotech Engineering Consultants, Ltd. 2009).

Borehole drilling and geophysical log

Five boreholes were drilled to depths ranging from 21 m to 39 m at the test site using a combination of mechanical and pneumatic drilling rigs with HQ bits (borehole diameter of 9.6 cm). Rock samples were collected at each borehole and allowed for an initial lithostratigraphic classification. The strata can be simply divided into three major geologic units: the surface sand-backfill layer (0 to 7.5 m), the sand/gravel layer (7.5 to 18.5 m), and the clay sandstone (18.5 to 40.0 m), respectively. The depth of the groundwater level was measured at 5 m below the surface.

The application of borehole geophysical log has long been widely considered in the field of hydrogeological investigations (Keys 1990; Helm-Clark *et al*. 2004; Hsieh *et al*. 2005). Both electrical log (ELOG) and sonic log (SLOG) were applied in this study. The ELOG was used to measure the natural gamma radiation (NGAM), single-point resistance (SPR), short and long-normal resistivity (SHN & LON). The SLOG was applied to detect the sonic travel time alone the borehole. Additionally, a temperature/conductivity log was also performed to measure the groundwater temperature and electrical conductivity gradient (difference per unit length) profile in the borehole. These are the useful techniques for locating the preferential flow path or the most permeable zone (Kayene *et al*. 1985; Keys 1990; Molina *et al*. 2002). The response of the geophysical log is shown in Fig. 2.

The NGAM log usually varies in close relation to the radiation emitted from the formation. It provides a constructive interpretation of the lithologic and stratigraphic classification (Keys 1990). According to the logging results, it was found that the formation is basically sandy. Three sections were found with relatively higher gamma radiation (from 24 m to 26.5 m, 28.5 m to 32 m, and 35 m to 37 m), which indicates that at these depths, larger amounts of fined-grained deposits (e.g. clay) were formed. The electrical resistivity signals showed a rightward shift at a depth of 10 to 18 m. Because the resistivity log generally increased with the grain size of the formation material (Keys 1990), it revealed that the specified section primarily consists of coarse-grained material (e.g. gravel). Besides, a significant separation between the SHN and LON was shown in the coarse grain dominated stratum. This is attributed to the fact that strong mud invention has occurred as a result of higher stratum permeability (Helm-Clark *et al*. 2004; Hsieh *et al*. 2005). Similar phenomena can be found from the SLOG, which displayed a longer travel time at the same domain. Inasmuch as the sonic velocity is porosity dependent, this segment was accounted for by the occurrence of cavities (or solution openings) associated with higher permeability. By comparison, the section below 18 m is mainly fine-grained, clay-dominated strata, and accordingly the permeability is relatively low. Such findings were supported by the temperature and conductivity log. A sharp deflection in both the temperature and conductivity gradient was observed from 10 m to 18 m, corresponding to the higher permeability of the sand and gravel stratum, while the deflection in clayey sandstone was not significant. The

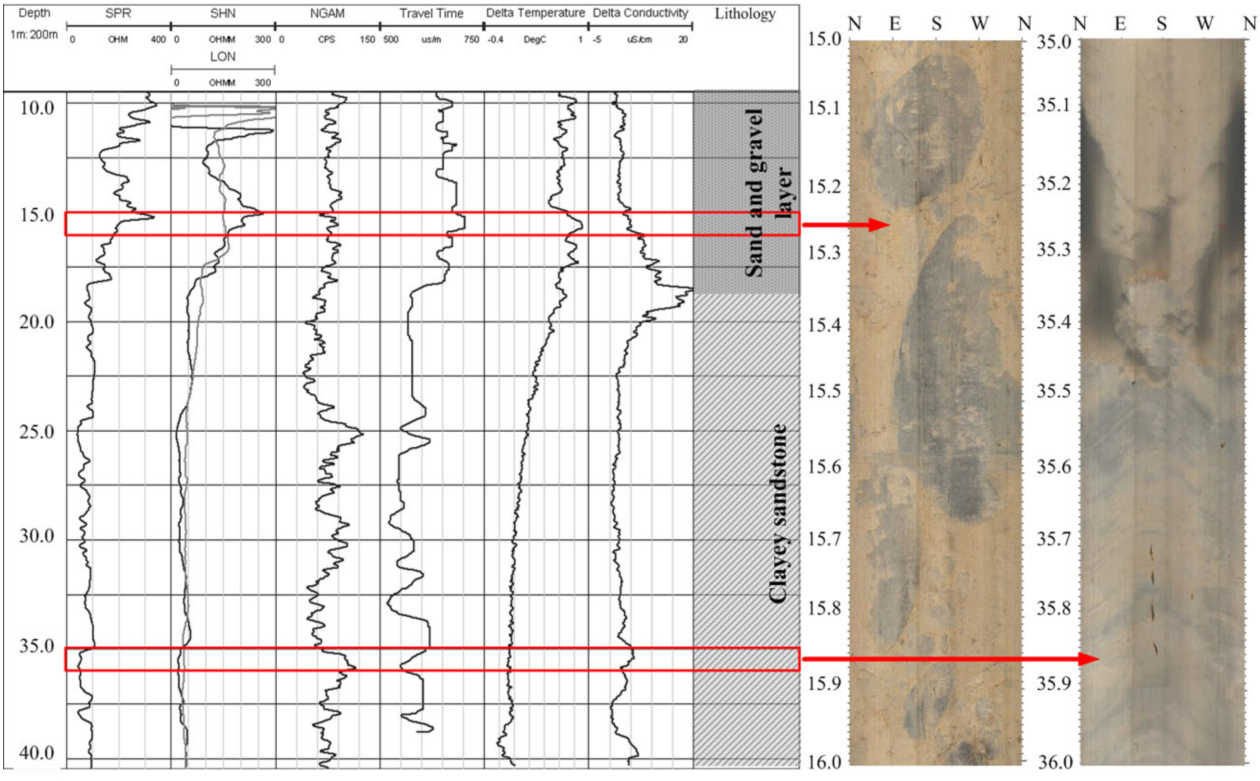

Fig. 2. Geophysical logging results (left); optical borehole image of sand and gravel stratum from 15~16 m, and clayey sandstone stratum from 35~36 m (right).

above-mentioned geological conditions and permeable interpretation based on borehole geophysical logging are highly consistent with the core data from drilling (Fig. 2).

Conjunctive use of pumping test and tracer test

Pumping tests and tracer tests have long been considered important for characterising aquifer hydraulic parameters including transmissivity, storativity and dispersivity (Oweis *et al*. 1990; Tonder *et al*. 2002; Lee *et al*. 2003; Niemann & Rovey 2009). The use of the two methods in conjunction enables the solute transport associated with the movement of groundwater at the test site to be temporarily controlled. The deployment of pumping and observation wells is shown in Fig. 3. The diameter of the pumping well NP1–5 is 15.2 cm, and the monitoring wells (NP1–6 to NP1–9) are 9.6 cm. The four monitoring wells were placed along the orthogonal lines that intersect NP1–5. The distance between wells was set at 5 m. The wells were completed by installing Polyvinyl Chloride (PVC) pipe casing (9.6 cm for pumping wells and 5.1 cm for observation wells) with a 12 m-long screen interval consisting of 0.25 mm slot openings in alternating positions. The position of the screen interval was selected based on the

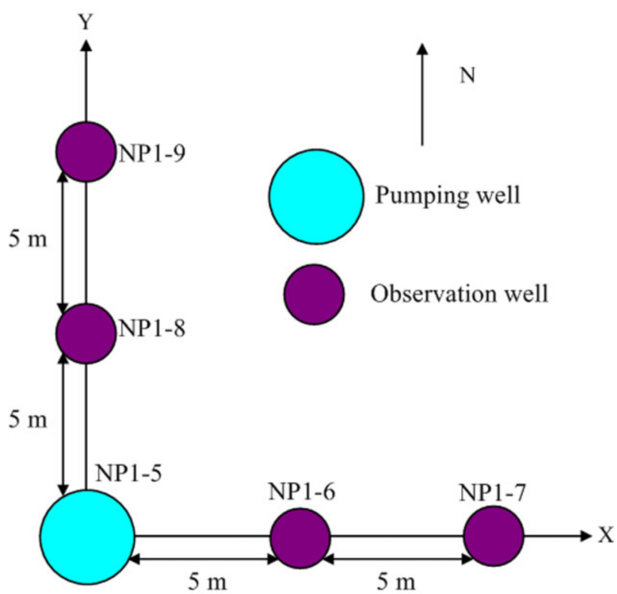

Fig. 3. Schematic drawing of well distribution.

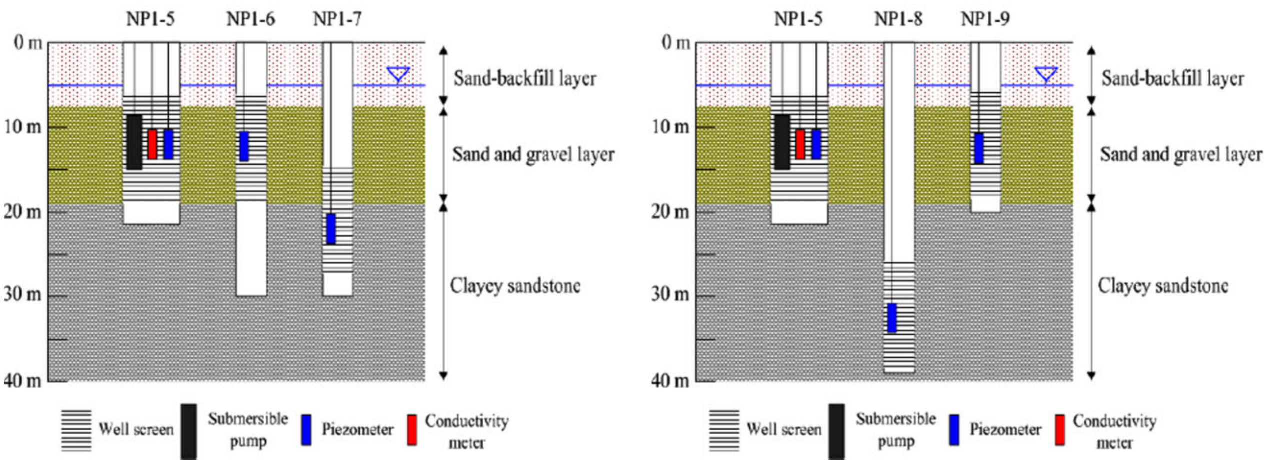

Fig. 4. Cross-sectional view in X-axis (left); and Y-axis (right) of test site.

Table 1 Well conditions and estimated hydraulic properties of pumping test

Well	Well type	Depth (m)	Screen interval (m)	Stratum	Diameter (cm)	Transmissivity (m^2/day)	Storage coefficient
NP1–5	Pumping	22	7–19	Sand and gravel	9.6	57.7	
NP1–6	Observation	30	6–18	Sand and gravel	5.1	20.3	3.68E-3
NP1–7	Observation	30	15–27	Interlayer	5.1	4.69	2.22E-3
NP1–8	Observation	39	26–38	Clayey sandstone	5.1	1.27	7.76E-3
NP1–9	Observation	21	6–18	Sand and gravel	5.1	57.5	1.84E-3

borehole geophysical logging data. As the cross-sectional view of the test site in Fig. 4 shows, a submersible pump and a conductivity meter were inserted in the pumping well. Piezometers were installed in all the wells to monitor the groundwater drawdown in different layers. The annular space surrounding the casing was filled with gravel-pack sand, and the annular space on the edge of the well screen was sealed with bentonite pellets. The overall well information is summarised in Table 1.

The pumping test was performed as designated by the American Society for Testing and Materials standard (ASTM D6034). During the test, water was extracted from the well with a constant pumping rate of 70 L/min and maintained for 24 h. The drawdown was measured every 30 s by the piezometers (Fig. 5). It was found that the drawdown observed in the sand and gravel stratum (NP1–5, NP1–6 and NP1–9) gradually stabilised after about 10 min. In comparison, the drawdown in the clayey sandstone (NP1–7 and NP1–8) continued to decrease. The difference may be that the sand and gravel stratum has higher transmissivity which provided more water and prevented the drawdown during pumping. The transmissivity and storage coefficient of the aquifer were determined via the drawdown data using AQTESOLV (Duffield 2004). In this study, the hydraulic properties were computed by adopting the analytical solution of

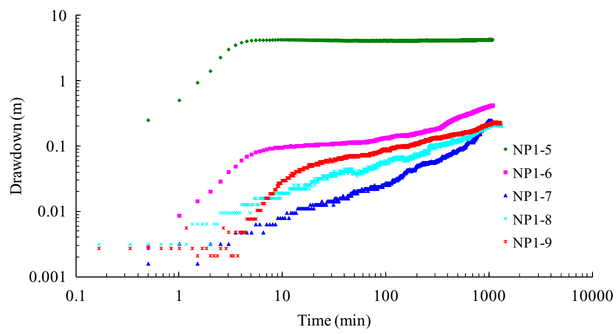

Fig. 5. Drawdown data of the pumping test.

Moench (1997). The drawdown and best type-curve matching data are shown in Fig. 6 and Table 1. The transmissivities of the sand and gravel stratum were calculated as 20.3 to 57.7 m^2/day, and 1.27 m^2/day in clayey sandstone. From comparison with the results of the borehole geophysical measurement, the transmissivities of the sand and gravel stratum are much greater than the estimates obtained in the clayey sandstone stratum. Clearly, the primary pathway for contaminant migration is deemed to be present in the shallow stratum. Consequently, the focus of the subsequent tracer test was on the sand and gravel stratum.

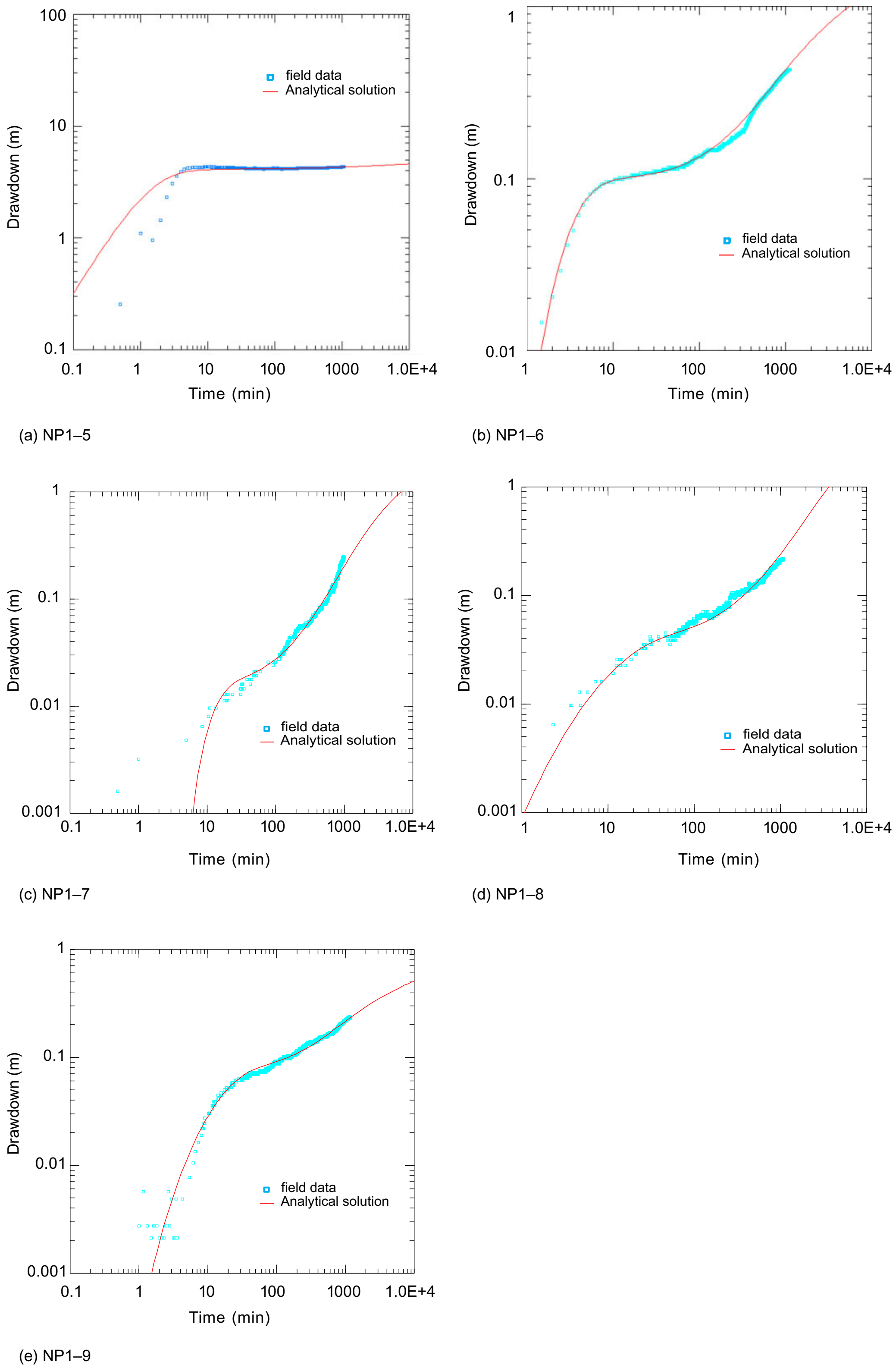

Fig. 6. Type-curve matching data of the pumping test in (a) NP1–5, (b) NP1–6, (c) NP1–7, (d) NP1–8, (e) NP1–9.

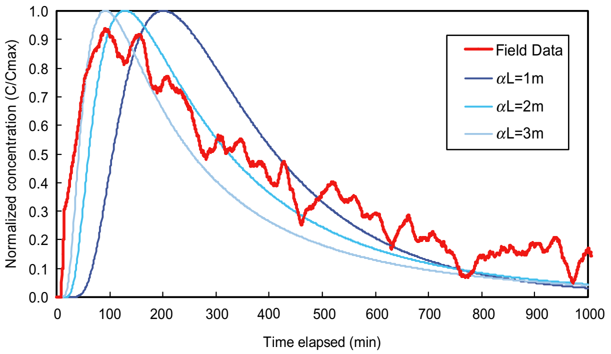

Fig. 7. The observed breakthrough curve and the computed curves with different dispersivity values using the analytical solution of Sauty (1980).

When groundwater level in the pumping well had stabilised, around 30 min after starting, 70 litres of sodium chloride (NaCl) solution with a concentration of 100 g/L was injected into the well NP1–6 through a PVC pipe. The concentration of the tracer solution was simultaneously measured in the pumping well (NP1–5) using a conductivity meter (Fig. 4). The data (known as the breakthrough curve) are shown in Fig. 7. Because the screen intervals were installed in the sand and gravel stratum for both the injection and pumping wells, the stratum dispersivity can be computed using an advection-dispersion solution for converging radial flow with a pulse tracer injection (Sauty 1980):

$$C(r,t)=\frac{\Delta M}{2Q\sqrt{\pi\alpha_L vt^3}}\exp\left[-\frac{(r-vt)^2}{4D_L t}\right] \quad (1)$$

where **C**(***r***, ***t***) is the concentration of the tracer in the injection borehole at time *t* (M/L^3); **Δ*M*** is the injected mass of the tracer per unit section (mass/thickness; M/L); $\boldsymbol{\alpha_L}$ is the longitudinal dispersivity (L); $\boldsymbol{D_L}$ is the longitudinal dispersion coefficient (= $\boldsymbol{\alpha_L} \times \boldsymbol{v}$; L^2/T); ***v*** is the groundwater velocity under forced gradient (i.e. the radial distance between two boreholes (***r***) over mean travel time; L/T); ***Q*** is the pumping rate of the well (L^3/T). The mean travel time can be obtained from the breakthrough curve using the following equation (Boggs & Adams 1992):

$$\bar{t}=\frac{\int_0^\infty C(t)t\,dt}{\int_0^\infty C(t)\,dt} \quad (2)$$

As shown in Fig. 7, the breakthrough curves obtained from the pumping well (in red) are compared with the empirical curves (in blue) derived by Sauty (1980). Although a periodic oscillation in concentration was shown as a result of the strong fluid disturbance by continuous water extraction, the optimal longitudinal dispersivity is found to range from 1 to 2 m in our case. The value obtained is fairly consistent with the results of Yang *et al*. (2002), who found that the longitudinal dispersivity in the sand and gravel aquifer was about 1.72 m. As the conductivity meter was installed in the pumping well, a better result would be achieved if measurements were made by collecting samples from the pumped water.

Conclusions

(1) Uncertainty associated with the measurement of *in situ* hydrogeological characteristics is a major factor in any environmental risk assessment.

(2) This paper presents a case study which illustrates a combination of hydrogeological investigation techniques that can provide greater certainty in the resulting measurement. This is particularly valuable when predicting containment flows from high-risk sites such as, in this instance, the Chin-Shan Nuclear Power Plant.

(3) The borehole electrical log, sonic log and groundwater temperature/conductivity log are ideal approaches that quickly identify the regional lithology and formation permeability. They are constructive for the evaluation of the potential pathway of contaminant migration.

(4) The combined use of interwell pumping and tracer test provides simultaneous estimation of multiple hydraulic parameters, including transmissivity, storage coefficient and dispersivity.

(5) The results not only clarify the complexities of *in situ* hydrogeological characteristics but also provide useful information to establish a reliable numerical model which simulates fluid and solute transport dynamics. In our opinion, the implementation of such *in situ* prospecting techniques is essential and necessary in assessing the environmental impact of a nuclear power plant site.

References

Boggs, J. and Adams, E. (1992) Field Study of Dispersion in A Heterogeneous Aquifer. *Water Resour. Res.*, **28**, 3325–3336.

Buchanan, D., Clark, C.F., Ferguson, N.S. and Kenny, M.J. (2001) Hydraulic Characteristics of Wet-Pulverised Municipal Waste. *Water Environ. J.*, **15**, 14–20.

Duffield, G.M. (2004) AQTESOLVE version 4 user's guide, Developer of AQTESOLV HydroSOLVE, Inc., Reston, VA, USA.

Helm-Clark, C.M., Rodgers, D.W. and Smith, R.P. (2004) Borehole Geophysical Techniques to Define Stratigraphy, Alternation and Aquifers in Basalt. *J. Appl. Geophys.*, **55**, 3–38.

Hsieh, B., Lewis, C. and Lin, Z. (2005) Lithology Identification of Aquifers from Geophysical Well Logs and Fuzzy Logic Analysis: Shui-Lin Area, Taiwan. *Comput. Geosci.*, **31**, 263–275.

Hsu, S.M., Lo, H.C., Jeng, D., Ku, C.Y. and Chi, S.Y. (2010) Integrating multiple subsurface exploration technologies in slope hydrogeologic investigation: a case study in Taiwan, ASCE Geotechnical Special Publication. 199, 980–989.

Hsu, S.M., Lo, H.C. and Chou, P.Y. (2011) Application of hydrogeological investigation to determine groundwater modeling approach in Taiwan mountainous region. In: 8th Asia Oceania Geosciences Society (AOGS) annual meeting. Taipei, Taiwan.

Kayene, I., Taniguchi, M. and Sanjo, K. (1985) Alternation of the Groundwater Thermal Regime Caused by Advection. *Hydrolog. Sci. J.*, **30** (3), 343–360.

Keys, S. (1990) *Borehole Geophysics Applied to Ground-Water Investigations. Techniques of Water-Resource Investigations of the United States Geological Survey*. Geological Survey, Denver, USA.

Ku, C.Y., Hsu, S.M., Chiou, L.B. and Lin, G.F. (2009) An Empirical Model for Estimating Hydraulic Conductivity of Highly Disturbed Clastic Sedimentary Rocks in Taiwan. *Eng. Geol.*, **109**, 213–223.

Lee, J.Y., Kim, J.W., Cheon, J.Y., Yi, M.J. and Lee, K.K. (2003) Combined Performance of Pumping and Tracer Test: A Case Study. *Geosci. J.*, **7**, 237–241.

Moench, A.F. (1997) Flow to A Well of Finite Diameter in A Homogeneous, Anisotropic Water Table Aquifer. *Water Resour. Res.*, **33**, 1397–1407.

Molina, L., Vallejos, A., Pulido-Bosch, A. and Sanchez-Martos, F. (2002) Water Temperature and Conductivity Variation As Indicators of Groundwater Behaviour in Complex Aquifer Systems in the South-East of Spain. *Hydrol. Process.*, **16**, 3365–3378.

Niemann, W. and Rovey, C. (2009) A Systematic Field-Based Testing Program of Hydraulic Conductivity and Dispersivity over A Range in Scale. *Hydrogeol. J.*, **17**, 307–320.

Oweis, I., Smith, D., Ellwood, R. and Greene, D. (1990) Hydraulic Characteristics of Municipal Refuse. *J. Geotech. Eng.*, **116**, 539–553.

Sauty, J. (1980) An Analysis of Hydrodispersive Transfer in Aquifers. *Water Resour. Res.*, **16** (1), 145–158.

Sinotech Engineering Consultants, Ltd. (2009) Site investigation and assessment of spent fuel dry storage plan in First Nuclear Power Plant. Taiwan Power Company, Ltd., Taiwan (in Chinese).

Tonder, G., Riemann, K. and Dennis, I. (2002) Interpretation of Single-Well Tracer Test Using Fractional-Flow Dimensions. Part 1: Theory and Mathematical Models. *Hydrogeol. J.*, **10**, 351–356.

Yang, Y.S., Lin, X.Y., Elliot, T. and Kalin, R. (2002) A Natural-Gradient Field Tracer Test for Evaluating of Pollutant-Transport Parameters in A Porous-Medium Aquifer. *Hydrogeol. J.*, **9**, 313–320.